P452 **_AVIATION APPLICATIONS OF A NEW GENERATION OF MESOSCALE NUMERICAL WEATHER PREDICTION SYSTEM OF THE HONG KONG OBSERVATORY_**

Wai-Kin WONG[*1], P.W. Chan[1] and Ivan C.K. Ng[2]
[1]Hong Kong Observatory, Hong Kong, China
[2]Hong Kong Polytechnic University, Hong Kong, China

1. INTRODUCTION

In June 2010, a new generation of mesoscale NWP system is operated by Hong Kong Observatory (HKO). It is called the Atmospheric Integrated Rapid-cycle (AIR) forecast model system based on the Non-Hydrostatic Model (NHM) of the Japan Meteorological Agency (JMA) (Saito *et al.* 2006), and its 3-dimensional variational data assimilation system (3DVAR), to replace the previous NWP system using Operational Regional Spectral Model (ORSM) system.

This paper presents performance and development of aviation application of AIR/NHM, including (i) verification results of wind forecasts against synoptic observations and aircraft wind data, (ii) development of turbulence intensity guidance and its verification using eddy dissipation rate (EDR) calculated from the flight recorder data of commercial aircraft. The verification results will also be compared with the turbulence products from the World Area Forecast Centres based on the global NWP models. Furthermore, on-going development in aviation weather forecast using AIR/NHM will also be discussed.

2. DESCRIPTIONS OF AIR/NHM

AIR/NHM has two domains, namely Meso-NHM and RAPIDS-NHM (Figure 1). Meso-NHM has horizontal resolution of 10 km and 50 terrain following vertical levels that provides 72-hour forecast updated at every 3 hours, using the boundary conditions from the JMA Global Spectral Model and daily sea-surface temperature analysis from the National Center for Environmental Prediction (NCEP). The horizontal grid-spacing of RAPIDS-NHM is 2 km and there are 60 vertical levels, RAPIDS-NHM analysis and forecast are executed every hour to provide storm-scale prediction over Hong Kong and its nearby Guangdong region up to 15 hours ahead. The boundary conditions are provided by Meso-NHM forecast in one-way nesting configuration. 3DVAR analysis is used to initialize the model forecast in both Meso-NHM and RAPIDS-NHM.

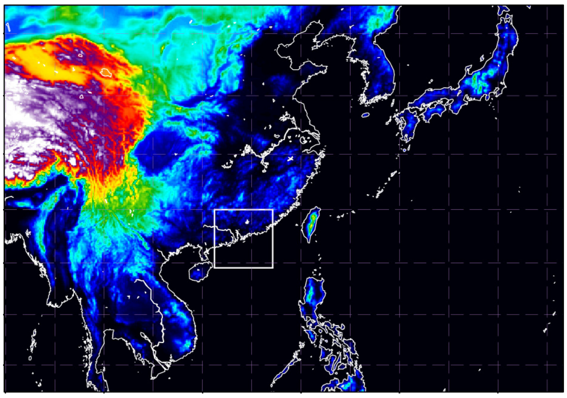

Fig. 1 Domains of Meso-NHM and RAPIDS-NHM (white square).

In both Meso-NHM and RAPIDS-NHM, 3DVAR analysis at full model resolutions and vertical levels is used in order to generate optimal initial condition containing the characteristics of synoptic and mesoscale circulations like the 3-dimensional distributions of momentum, temperature and moisture. Figure 2 shows an example of distribution of various observations assimilated in the 3DVAR analysis of Meso-NHM at 00 UTC, 21 October 2010. Meso-NHM 3DVAR can ingest various observational data including conventional data from synoptic stations, buoy and ships, aircraft (AMDAR - Aircraft Meteorological Data Relay), automatic weather stations over Hong Kong and Guangdong Province, wind profilers, atmospheric motion vector (AMV) from JMA MTSAT-1R/MTSAT-2, temperature retrieval profiles from NOAA polar-orbiting satellite and the total precipitable water vapour from microwave instruments. Tropical cyclone (TC) bogus data on surface pressure and 3-dimensional vortex wind profiles are ingested as additional observations when TC is analysed over the model domain. In RAPIDS-NHM, radar Doppler velocity and the total precipitable water vapour from the Global Positioning System (GPS) network over Hong Kong are also assimilated in the 3DVAR system.

* *Corresponding author address*: Wai-Kin WONG, Hong Kong Observatory, 134A, Nathan Road, Kowloon, Hong Kong, China; email: wkwong@hko.gov.hk.

(a)

(b)

(c)

(d)

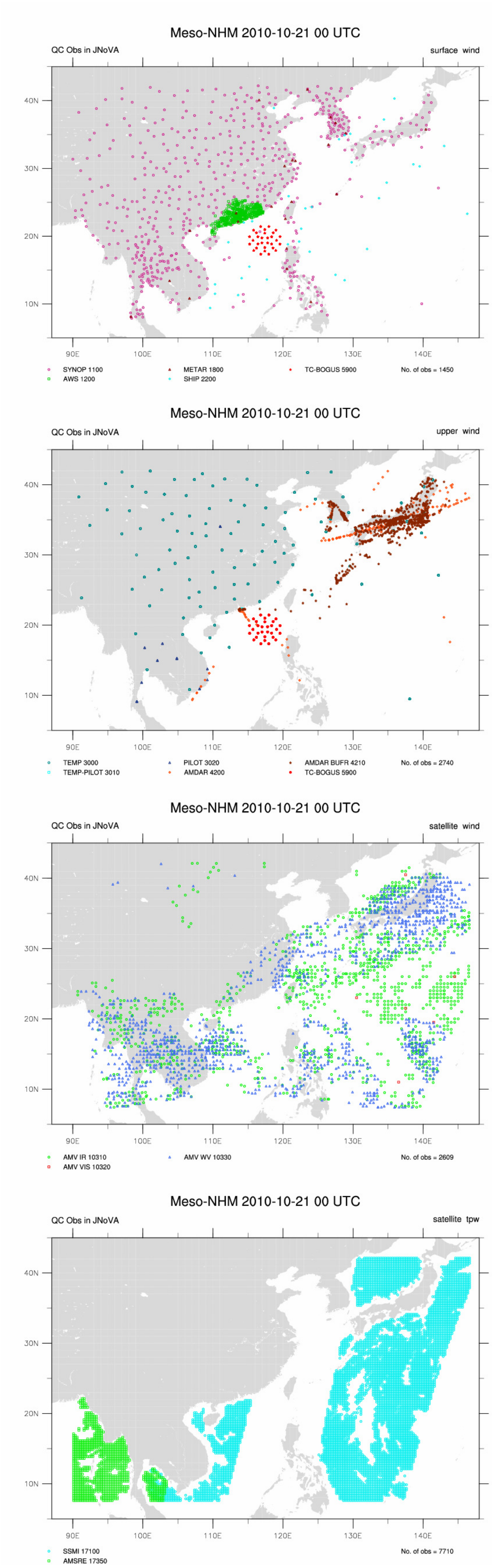

Fig. 2. Data ingested in Meso-NHM 3DVAR analysis at 00 UTC 21 October 2010 on: (a) surface wind, (b) upper-air wind, (c) MTSAT AMV, and (d) total precipitable water from SSM/I and AMSR-E.

3. PERFORMANCE OF AIR FORECAST MODEL SYSTEM

3.1 Verifications of meteorological elements

Through the ingestion of various observations, NHM is found to have substantial improvements over the previous ORSM system. Based on 50 selected surface and upper-air observation stations within the domain of Meso-NHM, monthly verification is carried out to study and monitor the performance of NHM. Figure 3(a)-(d) shows the time series of root-mean-square errors of mean-sea-level pressure, surface wind vector, temperature, and relative humidity from March to December 2010. Model analysis and forecast data at the nearest grid point from the station locations are used in the verification. RMSEs of analysis and forecasts at 24 hour intervals are denoted by different colours. Solid and dotted lines represent the verification statistics of Meso-NHM and ORSM respectively.

It can be seen that the RMSE of MSLP analysis is about 0.5 hPa and stays within 2.5 hPa throughout 72 hours of forecast, whereas the RMSE of MSLP for ORSM is about 1.2 hPa in the analysis and exceeds 3 hPa in 3-day forecasts. Using the u- and v- component of wind forecasts to compute the RMSE of surface wind vector, the RMSE for Meso-NHM 72-h forecast is within 7 knots, which is smaller than that of ORSM by about 1.5 knots. For temperature, the RMSE of Meso-NHM analysis is about 2 degrees and 72 hour forecasts is within 3 degrees. Improvements in the humidity analysis and forecasts are also seen in Meso-NHM as compared with ORSM. These substantial improvements probably attribute to the use of model surface process in the design of observation operator in 3DVAR to assimilate the surface meteorological elements in the initial condition, as well as the improved model physics to predict the surface weather elements.

From the verification of upper level wind, Meso-NHM also shows improvements over ORSM throughout the analysis and 3-day forecast period (Fig. 4). The reduction of error is about 10-15% in the 24-72 hours of forecasts from Meso-NHM.

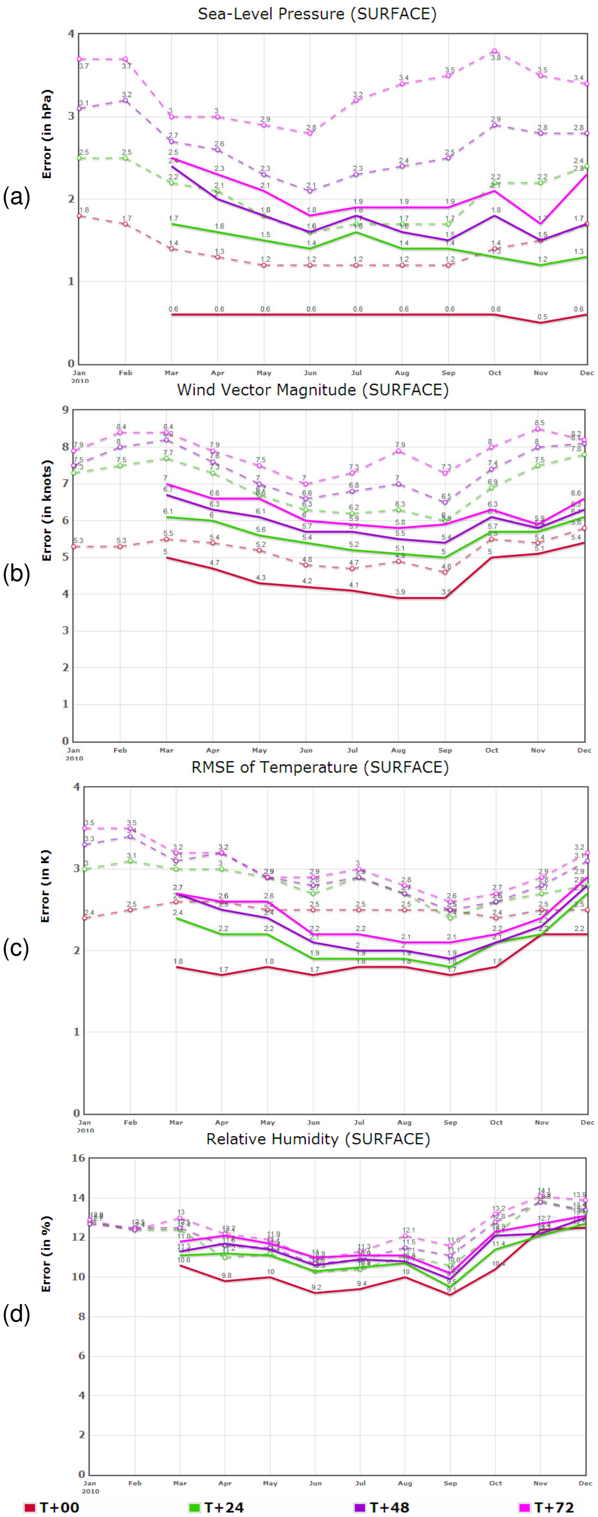

Fig. 3. RMSE of analysis and forecast of surface elements from Meso-NHM (solid lines) and ORSM (dotted lines) during Mar-Dec 2010 on (a) mean-sea-level pressure, (b) wind vector, (c) temperature and (d) relative humidity.

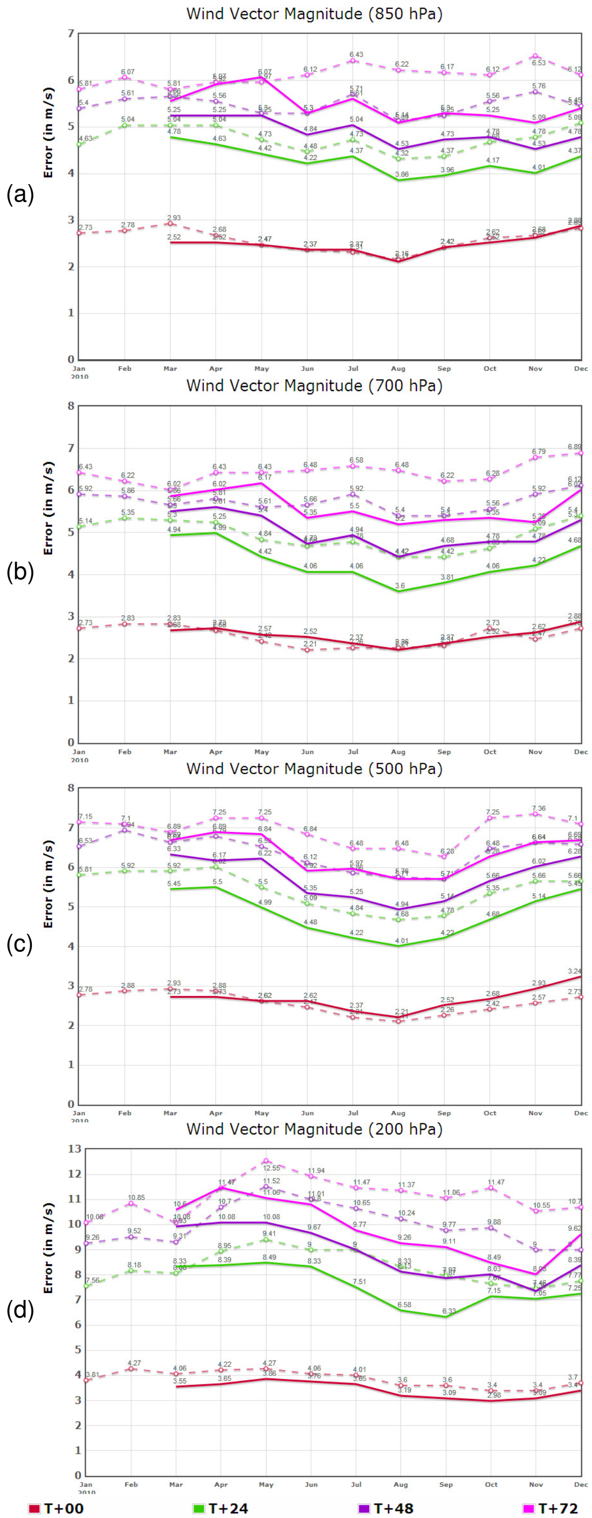

Fig. 4. RMSE of analysis and forecast of wind vectors from Meso-NHM (solid lines) and ORSM (dotted lines) during Mar-Dec 2010 on (a) 850 hPa, (b) 700 hPa, (c) 500 hPa and (d) 200 hPa.

3.2 Verification of wind forecast against AMDAR data

Two periods (May – Aug 2009, and Jul – Oct 2010) are chosen to study the performance of Meso-NHM and compare the verification statistics from other NWP models. In supporting the operation of arrival metering and sequencing in the Hong Kong International Airport, the NWP model products are used to produce gridded wind forecast on upper levels for the next 12 hours. AMDAR observations within 17-27N, 109-119E and between 150hPa and 1000hPa covering the Hong Kong Flight Information Region (HKFIR) are taken as the "sky truth". Gridded wind forecast data are interpolated to the time and position of aircraft observations for the verification.

From the verification statistics for May-Aug 2009 (Fig. 5(a)), Meso-NHM forecast (green line) shows improved performance compared to ORSM running at horizontal resolution of 60 km (blue) and 20 km (purple) as the RMSE of vector wind error is in general reduced by 0.5-1 m/s, and performs similarly to the JMA global model forecast (red). For Jul – Oct 2010 (Fig. 5b), the performance of Meso-NHM is also on-par with the both JMA (red) and ECMWF (blue) forecasts.

(a)

(b)

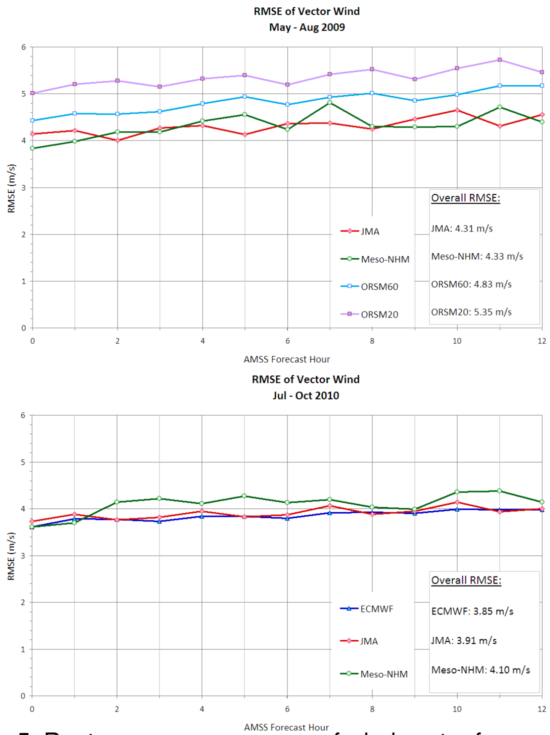

Fig. 5. Root-mean-square errors of wind vector forecasts (in m/s) from various NWP models for (a) May-Aug 2009, and (b) Jul-Oct 2010.

4. DEVELOPMENT OF TURBULENCE FORECAST GUIDANCE

4.1 Turbulence index

To enhance the support in the preparation of aviation significant weather chart and the issuance of en-route turbulence warning, experimental turbulence intensity guidance product from Meso-NHM has been developed. Turbulence index (TI) on selected flight levels is generated to consider effects due to vertical wind shear, horizontal wind deformation and convergence.

$$TI = \frac{|\Delta \mathbf{V}|}{\Delta z} \times \sqrt{\left(\frac{\partial u}{\partial x} - \frac{\partial v}{\partial y}\right)^2 + \left(\frac{\partial v}{\partial x} + \frac{\partial u}{\partial y}\right)^2} - \left(\frac{\partial u}{\partial x} + \frac{\partial v}{\partial y}\right)$$

To account for effects due to gravity wave generation in cyclonic areas and anticyclonic flow, tendency of horizontal divergence at two forecast times is added to TI to formulate another turbulence index called DTI (Ellrod and Knox, 2010):

$$DTI = TI + \beta \times \left[\left(\frac{\partial u}{\partial x} + \frac{\partial v}{\partial y}\right)\Big|_{T2} - \left(\frac{\partial u}{\partial x} + \frac{\partial v}{\partial y}\right)\Big|_{T1}\right]$$

4.2 Verification against aircraft data

Both TI and DTI demonstrate forecasting skills in capturing moderate turbulence level or above, as seen from verification using eddy dissipation rate (EDR) calculated from wind data of commercial jets as the "sky-truth". Various thresholds of forecast TI and DTI from NHM over 0.1x0.1 degree grid box during May-August 2009 are verified against the "sky-truth" with maximum EDR ≥ 0.4 $m^{2/3}s^{-1}$ representing moderate turbulence level or above for the peak turbulence encountered. TI and DTI attained a hit rate of about 0.5 for a false alarm of 0.35 (Fig. 6) for 6-12 hours of forecasts. It is found that the performance of TI and DTI from NHM is similar to that of turbulence potential product from the World Area Forecast Centres based on UK (Wong et al. 2011).

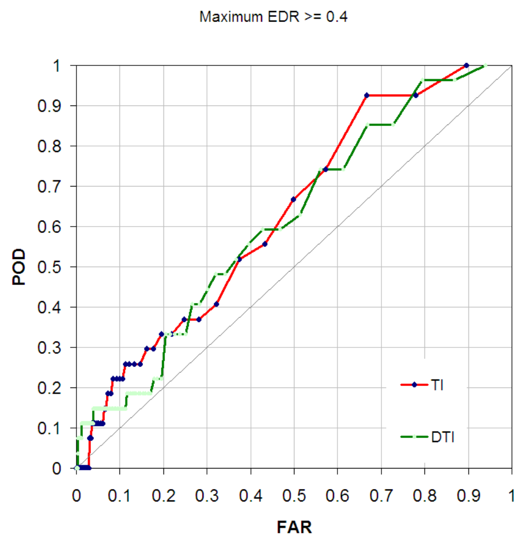

Fig. 6. Relative operating characteristics curves of TI and DTI forecasts from NHM.

5. OTHER DEVELOPMENT OF AVIATION APPLICATIONS USING AIR/NHM

Development is underway to apply both Meso-NHM and RAPIDS-NHM to support aviation weather forecasting in respect like visibility level and significant convection to support aerodrome forecast application. For the latter, the use of nowcast-NWP blending technique (Wong et al. 2009) shows promising performance as seen from rainstorm cases.

In late evening on 8 September 2010 to the following early morning, widespread thunderstorms and significant convection affected the coastal regions of Guangdong and Hong Kong due to development of convection over inland areas arising from prolonged daytime heating. From successive RAPIDS-NHM runs initialized during the afternoon on 8 September (Fig. 7), intense precipitation is forecast to develop over Guangdong coastal area and later affects Hong Kong and Pearl River Delta region. The indication on the convective development during the overnight period is consistent based on forecasts from successive model runs, though the timing on the passage of severe thunderstorm lags behind the actual situation by about 2 hours, probably due to spin-up time required for the model. With further development in data assimilation and forecast model, the spatial-temporal error of model quantitative precipitation forecast (QPF) associated with severe convective system could be further reduced. Moreover, through the use of an optimal phase correction technique, the model QPF can provide useful guidance on the development of significant precipitation through the blending with nowcast QPF based on extrapolation technique of radar imagery (Wong et al. 2009). Fig. 8(a)-(b) shows the T+5 hour radar nowcast QPF and blending QPF at 01HKT on 9 September (17 UTC, 8 September). It is clearly seen that RAPIDS-NHM provides signs of significant rainfall over HK during 00-01 HKT. The phase correction is applied to relocate the model QPF pattern when radar imagery is made available every 6 minutes. In this case, the blending output is also found to give a consistent scenario on the significant precipitation over Hong Kong during the overnight period. Further development will be conducted to study the techniques to improve both model forecast and blending algorithm, in order to enhance the capability in forecasting significant convection to support both aviation and public weather services.

(a)

(b)

(c)

(d)

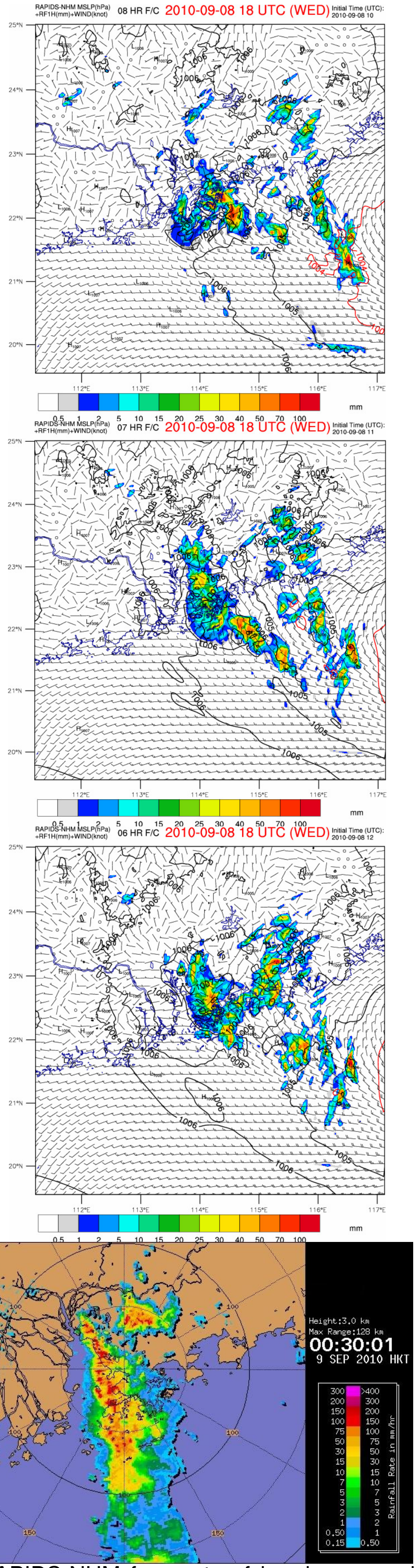

Fig. 7. RAPIDS-NHM forecasts of hourly accumulated rainfall and mean-sea-level pressure at 02:00 HKT 9 September 2010, with model runs initialized from 10 to 12 UTC 8 September shown in (a)-(c) respectively; radar reflectivity image at 00:30 HKT 9 September 2010 shown in (d)

(a)

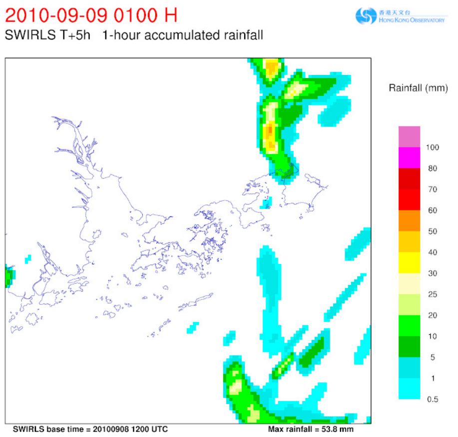

(b)

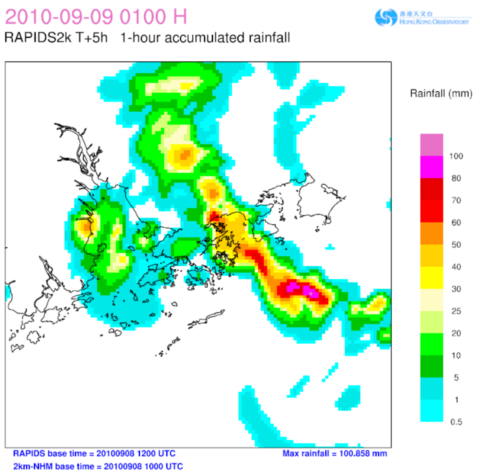

Fig. 8. (a) QPF on 1-hour accumulated rainfall ending at 0100 HKT 9 September 2010 using radar extrapolation techniques; (b) Blending QPF by combining radar nowcast and phase corrected RAPIDS-NHM forecast.

6. SUMMARY

The new operational NWP system using NHM shows improved performance in forecast of meteorological elements.

NHM demonstrates promising forecast skills in upper air winds and turbulence intensity that facilitates the NWP support in operational aviation weather forecasting. Development of more aviation-specific model products will be made to enhance the support in future aviation applications and weather services.

Acknowledgement

The authors would like to thank Mr. C.K. Chow, Mr. C.H. Lam and Mr. W.L. Li for the preparation of the verification statistics. AIR/NHM is developed on the basis of the NPD/MRI Non-Hydrostatic Model of the Japan Meteorological Agency.

Reference

Ellrod, G. P., J. A. Knox, 2010: Improvements to an Operational Clear-Air Turbulence Diagnostic Index by Addition of a Divergence Trend Term. Wea. Forecasting, 25, 789–798.

Saito, K., T. Fujita, Y. Yamada, J. Ishida, Y. Kumagai, K. Aranami, S. Ohmori, R. Nagasawa, S. Kumagai, C. Muroi, T. Kato, H. Eito, and Y. Yamazaki, 2006: The Operational JMA Nonhydrostatic Mesoscale Model. Mon. Wea. Rev., 134, 1266-1298.

Wong, W.K., P.W. Chan and C.M. Li, 2011: Verification of NWP turbulence intensity guidance using eddy dissipation rate from aircraft data. 24th Conference on Weather and Forecasting/20th Conference on Numerical Weather Prediction, American Meteorological Society, Seattle, USA, 24-27 Jan 2011.

Wong, W.K., L.H.Y. Yeung, Y.C. Wang and M. Chen, 2009 : Towards the Blending of NWP with Nowcast — Operation Experience in B08FDP, WMO Symposium on Nowcasting, 30 Aug-4 Sep 2009, Whistler, B.C., Canada.